

# Geometry of Double Retrograde Vaporization

## Prediction

G. B. Libotte,<sup>†</sup> F. D. Moura Neto,<sup>†,‡</sup> L. F. C. Jatobá,<sup>†</sup> C. N. Parajara,<sup>†</sup> and G. M.

Platt<sup>\*,†</sup>

<sup>†</sup>*Polytechnic Institute, Rio de Janeiro State University, Nova Friburgo, Brazil*

<sup>‡</sup>*Instituto de Matemática Pura e Aplicada, Rio de Janeiro, Brazil*

E-mail: [gmplatt@iprj.uerj.br](mailto:gmplatt@iprj.uerj.br)

Phone: +55 (22)25192166

### Abstract

Double retrograde vaporization is a phase behavior phenomenon that occurs close to the critical point of binary mixtures, characterized by wide relative difference of volatility between its components. In general, the phenomenon occurs in a very narrow composition range, making the prediction of the molar fraction and pressure of the phase equilibrium problem a challenging problem. Here we employ sophisticated modern numerical methodology to untangle the geometry of this complex phenomenon, based on the robust methodology of inversion of functions. The objective of this work is to evaluate the system that describes the phenomenon close to the singularity points of the problem, especially with respect to the degeneration of solutions. The method used offers an effective framework for the qualitative analysis of systems of nonlinear equations. We study an application of this methodology in the binary system formed by ethane + limonene, at three different configurations (four dew points, three dew points and only one dew point). The results indicate a very complex structure of the function in the neighborhood of the phenomenon.

# Introduction

Double retrograde vaporization is a phase behavior phenomenon that occurs close to the critical point of binary mixtures, that is, the point where there are no phase boundaries and therefore the distinction between them does not exist, causing the mixture to cease to exist as well. It occurs in mixtures characterized by involving a solvent with high volatility relative to the solute contained in the mixture. More specifically in relation to the mixture to be studied, composed of ethane + limonene, the solvent boils at 184.6 K, while the boiling point of the solute is 448.2 K. This tendency towards evaporation of ethane in relation to limonene causes its volatility to be high, satisfying one of the conditions of occurrence.

The phenomenon corresponds to a special shape of the dew-point curve, exhibiting a “S” shape (with three dew points) or a double-dome structure (with four dew points), for specific system temperature and composition. Especially in the case of double-dome manifestation, the phenomenon occurs within a very limited temperature range, which is slightly above to the critical temperature of the more volatile component. We must mention that the composition of vapor phase is arbitrarily chosen, in order to produce the thermodynamic phenomenon.

Its occurrence was firstly investigated by Chen et al.<sup>1</sup> and Chen et al.<sup>2</sup> for binary mixtures involving methane + n-butane and methane + n-pentane, under specified temperature. More recently, Raeissi and Peters<sup>3</sup> identified a double-dome behavior for the binary mixture ethane + limonene at  $T = 307.4$  K and in a narrow range of compositions (close to the pure ethane). Furthermore, Raeissi and Peters<sup>4</sup> indicated that the Peng-Robinson equation of state<sup>5</sup>, with classical mixing rules, was capable to qualitatively predict this phenomenon. In order to detail the thermodynamic fundamentals of double retrograde vaporization, Raeissi and Peters<sup>6</sup> also presented a detailed discussion of the volumetric properties of the fluids involved as defining the existence of the phenomenon.

In the vicinity of the mixture critical point, the robust calculation of dew point pressures (under specified temperature) is a very hard task. Furthermore, some roots of the phase

equilibrium problem show very small radius of convergence for Newton-type methods, as indicated by Platt et al.<sup>7</sup>. For this reason, the development of robust frameworks for this type of problem is extremely relevant. Among several possibilities, we focus on the robust methodology of the numerical inversion of functions, proposed by Malta et al.<sup>8</sup>, where they developed an extensive theory to handle functions in a generic class of functions defined in the whole plane to the plane. Their theory give precise statements about the solution of 2 by 2 systems of nonlinear equations, when the function is defined everywhere in the plane. From their theory we select a few techniques which are applicable to our thermodynamic problem, namely, this technique<sup>8</sup> proposes — considering a generic class of functions — the computation of critical curves in the mathematical sense<sup>1</sup>, the construction of a bank of solved points (to be used as with good initial estimates for all the possibly multiple solutions) and, finally, the inversion of the desired point (calculation of all pre-images of a such image).

As far as we know, the first application of these techniques of the general methodology of numerical inversion of functions from the plane to the plane, adapting them to handle a chemical engineering problem, was presented by Guedes et al.<sup>9</sup>, in the prediction of the azeotropic behavior in systems with double azeotropes. More recently, Libotte et al.<sup>10</sup> presented some preliminary results regarding the application of the methodology proposed by Malta et al.<sup>8</sup> in the prediction of double retrograde vaporization phenomenon in the system ethane + limonene.

In addition to being a robust framework in the resolution of nonlinear systems, the method of inversion of functions from the plane to the plane provides relevant information that allows a deeper analysis of the function studied. Some aspects are fundamental for understanding the behavior of the function from a global perspective. Among these aspects, we can briefly mention: (i) the influence of the system temperature in the critical curves, and (ii) the analysis of the behavior of inversions near the critical image (where the number

---

<sup>1</sup>The term “critical” assumes two meanings in this work: in the mathematical sense, a critical point of a function is a non-regular point (where the Jacobian matrix is non-invertible); in the thermodynamic sense, the critical point is that where we cannot distinguish between the properties of the phases.

of pre-images — solutions of the system — change). As pointed previously, the solution of this kind of nonlinear system with typical derivative based root-finding algorithms (such as Newton's methods) is not a trivial task, even when using more sophisticated numerical tools<sup>7</sup> and thus, one of the objectives of this work is to provide a geometrical view of this challenging nonlinear algebraic system, which can be useful in the development of numerical tools for solving high-pressure phase equilibrium problems.

In order to analyze these main points and provide an in-depth geometric study of the phase equilibrium problem in two-component systems, we present two case studies. The first one is the system composed of ethane + limonene at  $T = 307.4$  K which is analyzed, fixing the molar fraction of the vapor phase of ethane at  $y_1 = 0.998966$ . Under these conditions, the system presents four distinct solutions, corresponding to the intersections of the dew point curve with the line of a given mole fraction, as can be seen in Figure 1. For this system, all the steps of the method of inversion of functions from the plane to the plane were performed and the solution degeneration was investigated by obtaining pre-images of a set of points located in the vicinity of the critical image. We also evaluated the critical points of the function that defines the nonlinear system that are folds and cusps, and their relation with the degeneration of solutions of this problem.

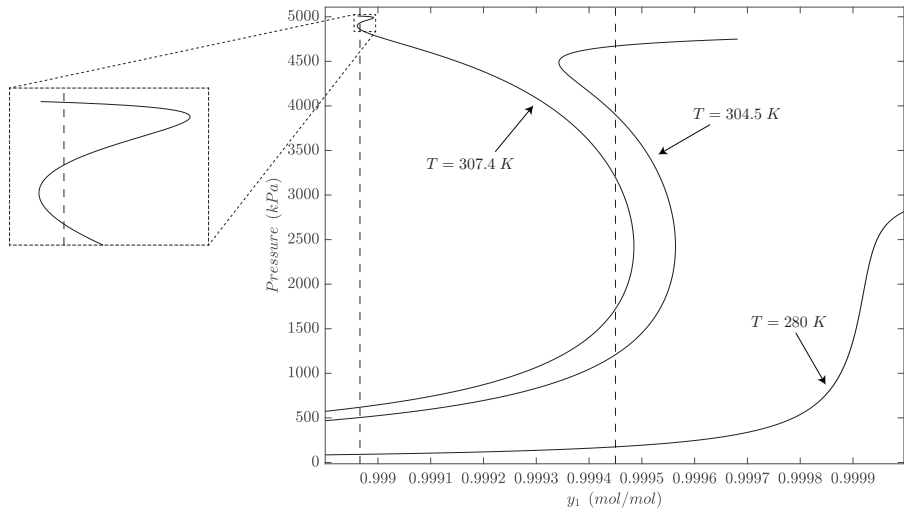


Figure 1: Dew point curves for the system ethane + limonene at several temperatures.

In the second case study, the temperature of the system composed of the same components of the previous case was set at  $T = 304.5$  K and compared with the same system at  $T = 280$  K. In these temperature scenarios, with  $y_1 = 0.99945$  (among other conditions), the system has three and one solutions, respectively, as shown in Figure 1. Thus, it is possible to evaluate the degeneracy of solutions in both systems, varying only one of the parameters of the problem.

The possibility of solving the problem — and therefore obtaining the pre-images of a given point in the image — was also evaluated from a mathematical perspective: the critical curves of the function defining the nonlinear system were obtained for different temperatures and their respective critical images. Through this variation, for a fixed molar fraction of ethane in the vapor phase, it was possible to verify the influence of the critical curves in obtaining the solutions of the problem through methods that use derivatives.

The remaining of this work is organized as follows. First we discuss the thermodynamic model. Next we present the mathematical and numerical methodology, beginning with an example of a scalar function of one variable (1D case) and showing how the critical points and their images are used to break the equation in cases where the number of solutions is constant, followed by a discussion of functions of two variables (2D case), and fold and cusp critical points. The construction of the critical set and of the bank of solved problems is next. Finally we present and discuss the numerical examples, and conclusions.

## Models and Methodology

### Thermodynamic models and problem formulation

All the phase equilibrium calculations, as well as the critical point curves (in the thermodynamic sense), are conducted for the Peng-Robinson equation of state<sup>5</sup> with classical mixing rules and null binary interaction parameters. Critical properties and acentric factors of pure components can be found, for instance, in Libotte et al.<sup>10</sup>.

For a binary mixture, the phase equilibrium problem can be formulated as:

$$\hat{\phi}_i^L x_i = \hat{\phi}_i^V y_i , \quad i = 1, 2 . \quad (1)$$

In the last equation,  $\hat{\phi}$  represents the fugacity coefficient for component  $i$  (using the Peng-Robinson model with classical mixing rules),  $x_i$  is the molar fraction in the liquid phase and  $y_i$  represents the vapor phase. The superscripts  $L$  and  $V$  refer to the liquid and vapor phases, respectively.

Using  $x_2 = 1 - x_1$  and  $y_2 = 1 - y_1$ , the nonlinear algebraic problem (in the plane) is then:

$$\hat{\phi}_1^L x_1 = \hat{\phi}_1^V y_1 , \quad (2a)$$

$$\hat{\phi}_2^L (1 - x_1) = \hat{\phi}_2^V (1 - y_1) . \quad (2b)$$

The vector of unknowns, considering the specification of temperature and vapor molar fractions, is  $p = (x_1, P)$ . Let the residue of the nonlinear equations be denoted by  $f_i$ , and define  $F = F(x_1, P) = (f_1, f_2) = (\hat{\phi}_1^L x_1 - \hat{\phi}_1^V y_1, \hat{\phi}_2^L (1 - x_1) - \hat{\phi}_2^V (1 - y_1))$ . Thus, in general, the nonlinear algebraic system can be re-stated as

$$F(p) = q , \quad (3)$$

where  $p$  is a point in the domain and  $q$  is a point in the image (range) of  $F$ . Ordinarily, we are interested to solve  $F(p) = (0, 0)$  (where  $q = (0, 0)$  represents the null vector in the Euclidean plane).

## Some features of the numerical inversion of functions

Here we present a few fundamental ideas on the solution of a nonlinear system by numerical inversion of the associated functions.

## A 1D example

To get a grasp of the methodology of inversion of functions to solve nonlinear systems of equations, we first consider a simple 1D example. Let  $F(p) = p^3 - 3p^2 + 2p = p(p-1)(p-2)$ . Assume that for physical reasons  $p$  is always non-negative. By examining the graph of  $F$  it is possible to check that the equation for  $p$ , depending on  $q$ ,  $F(p) = q$ , that is,  $p^3 - 3p^2 + 2p = q$ , has 0 to 3 solutions. If  $\eta(q)$  denotes the number of solutions as a function of  $q$ , then,

$$\eta(q) = \begin{cases} 0, & \text{if } q < -2\sqrt{3}/9 \\ 1, & \text{if } q = -2\sqrt{3}/9 \text{ or } q > 2\sqrt{3}/9 \\ 2, & \text{if } -2\sqrt{3}/9 < q < 0 \\ 3, & \text{if } 0 \leq q < 2\sqrt{3}/9 \end{cases}.$$

The jumping points, where the number of solutions can change, are either the image of a critical point — a critical image — or an image of a boundary point of the domain of definition of  $F$ . The critical points (where the derivative is zero) satisfy  $F'(p) = 3p^2 - 6p + 2 = 0$ , that is  $p = 1 \pm \sqrt{3}/3$ . Since 0 is the only boundary point of the domain, the jumping points are  $F(1 \pm \sqrt{3}/3) = \mp 2\sqrt{3}/9$  and  $F(0) = 0$ . These points suggest a partition of the range of  $F$  in seven subsets,  $\mathbb{R} = \mathcal{T}_1 \cup \mathcal{T}_2 \cup \mathcal{T}_3 \cup \mathcal{T}_4 \cup \mathcal{T}_5 \cup \mathcal{T}_6 \cup \mathcal{T}_7$ ,

$$\begin{aligned} \text{jumping sets} \quad & \mathcal{J}_2 = \left\{ -\frac{2\sqrt{3}}{9} \right\}, \quad \mathcal{J}_4 = \{0\}, \quad \mathcal{J}_6 = \left\{ \frac{2\sqrt{3}}{9} \right\} \\ \text{tile sets} \quad & \mathcal{T}_1 = \left] -\infty, -\frac{2\sqrt{3}}{9} \right[ , \quad \mathcal{T}_3 = \left] -\frac{2\sqrt{3}}{9}, 0 \right[ , \quad \mathcal{T}_5 = \left] 0, \frac{2\sqrt{3}}{9} \right[ , \quad \mathcal{T}_7 = \left] \frac{2\sqrt{3}}{9}, +\infty \right[ \end{aligned}$$

Note that the number of solutions is constant in each tile. The overall strategy for solving the equation  $F(p) = q$  is to compute the jumping sets and, by taking the complementary set, decompose the range of  $F$  in its jumping and tile sets, have a bank of solved points with representatives more or less covering all the tile sets, and to solve the equation with the bank of solved points providing initial guesses for each solution.

## Jumping and tiles in the 2D case

Now we consider  $2 \times 2$  systems of equations,  $F(p) = q$ , with  $q \in \mathbb{R}^2$  and  $F$  a function defined on a subset  $\Omega$  of the plane to the plane,  $F : \mathbb{R}^2 \supset \Omega \rightarrow \mathbb{R}^2$ . Recall that the Jacobian  $JF|_p$  at a point  $p = (x, y) \in \mathbb{R}^2$  is

$$JF|_p = \begin{pmatrix} \frac{\partial f_1}{\partial x} & \frac{\partial f_1}{\partial y} \\ \frac{\partial f_2}{\partial x} & \frac{\partial f_2}{\partial y} \end{pmatrix}.$$

A point  $p$  in the domain is said a critical point if  $JF|_p$  is not invertible, which is equivalent to say that  $\det(JF|_p) = 0$ . A critical point is non-degenerate if  $\text{grad}(\det(JF|_p)) \neq 0$ . Under such conditions, the Jacobian matrix is not the null matrix. Therefore, this matrix has rank equal to one in  $p$  and there is a nonzero vector that is tangent to the critical curve. As a consequence, if a function has only non-degenerate critical points — which we assume — their set is formed by curves, the critical curves,

$$\mathcal{C} = \{p \in \mathbb{R}^2 \mid \det(JF|_q) = 0\},$$

and the image of  $\mathcal{C}$ ,  $F(\mathcal{C}) = \{q = F(p), \text{ for all } p \in \mathcal{C}\}$ , is called the critical image. The set formed by the union of the critical image and the image of the boundary of the domain of  $F$ ,  $\mathcal{J} = F(\mathcal{C}) \cup F(\Omega)$ , define the jumping curves. The tiles are the connected components on the complement of  $\mathcal{J}$ ; if there are  $k$  connected components,  $\mathcal{T}_i$ , then  $\mathbb{R}^2 = (\cup_{i=1}^k \mathcal{T}_i) \cup \mathcal{J}$ , just as in the 1D example. The number of solutions of the equation  $F(p) = q$  is constant if  $q \in \mathcal{T}_i$ , and may jump when crossing  $\mathcal{J}$ .

One of the drawbacks to the application of the detailed theory presented in Malta et al.<sup>8</sup> to problems coming from applications that involve the solution of nonlinear  $2 \times 2$  systems of equations is not so much that it applies only to a special collection of functions, but that the functions have to be defined in all points in the plane. When that happens, the theory gives a fairly good amount of information on the solutions of the nonlinear system of equations. In applications, however, the domain of a function has to satisfy some restrictions due, for

instance, to the lack of physical significance of certain values of the variables, or due to existence of singularities, which breaks the theory presented in Malta et al.<sup>8</sup>. This is the case in the problems we are considering since, *e.g.*, the volume cannot be less than a certain quantity, and the pressure cannot be above certain critical value. Nonetheless the overall methodology that they discuss is preserved in the form of algorithms.

### The inversion of functions from the plane to the plane

Next, we present the method of inversion of functions from the plane to the plane, as well as the main definitions that support the technique. A detailed description of the method can be found in Malta et al.<sup>8</sup>.

The method is intended to solve systems with two equations and two unknowns of type  $F(p) = q$  with  $p, q \in \mathbb{R}^2$  and  $F$  should be a smooth function. In dealing specifically with critical points, they are assumed of just two types, either folds or cusps. Folds and cusps are non-degenerate critical points such that near them, and by means of differentiable changes of variables in the domain and in the image, they can be written, respectively, as  $(x, y) \mapsto (x, y^2)$ , and  $(x, y) \mapsto (x, y^3 \pm xy)$ , near the origin.

Following Malta et al.<sup>11</sup>, a fold is a non-degenerate critical point such that the kernel  $K$  of the Jacobian and the tangent line  $T$  to the critical set in  $p$  do not coincide. When they do coincide, and another criterion of non-degeneracy is satisfied,

- for a smooth parametrization  $\gamma : (-\epsilon, \epsilon) \rightarrow \mathbb{R}^2$  of  $C$  near  $p$ , with  $\gamma(0) = p$  and  $\gamma'(0) \neq 0$ , the angle  $\theta(\gamma(t))$  between the kernel  $K(\gamma(t))$  of  $JF(\gamma(t))$  and the tangent line  $T(\gamma(t))$  to  $C$  satisfies  $\theta'(0) \neq 0$ ,

the critical point is a cusp.

Within the scope of functions from the plane to the plane, we must introduce two descriptions of very important type of functions. A continuous function from a subset of the plane to the plane is proper if  $\lim_{|(x, y)| \rightarrow \infty} |F(x, y)| = \infty$ . This avoids to treat equations with infinitely many solutions. A 1D case, of an equation with infinite solutions, is  $\sin x = 0$ .

This happens because  $\sin x$  is not a proper function. In turn, a smooth proper function from the plane into itself is excellent if every critical point of  $F$  is a fold or a cusp. In essence, the theory developed in Malta et al.<sup>8</sup> aims at solving equations defined by excellent functions that satisfy yet another technical condition, the nice functions. For them, the theory asserts several results. An essential feature of the class of nice functions is that, under a suitable topology, they are generic in a mathematical sense. That means in particular that they are an open set. From a simplified point of view, that property expresses that any smooth function can be approximated arbitrarily close by a nice function. Therefore, the analysis can be restricted to this type of function. That is, in practice, it is enough to work with nice functions, thus the critical points are only cusps and folds.

The methodology of inversion of functions from a subset of the plane to the plane is composed of three fundamental steps: obtaining the critical set of  $F$ , creating the bank of solved points and calculating the pre-images from an arbitrary point. Each of these steps will be described next.

### **Generation of the critical set**

Knowing the critical set is fundamental in the inversion process, since it allows the computation of the critical image which, as illustrated in the 1D example, are places where the number of solutions may change — in these cases we say that the solutions degenerate. In addition to tracing the regions where the continuation method does not encounter points of singularity in the inversion process, it also indicates the boundary of the different tiles, which is a primordial concept in the analysis of solution degeneration.

In the original procedure, Malta et al.<sup>8</sup> proposes various calculations and verifications in order to establish that, strictly speaking, the critical points obtained form the critical set as a whole. In addition, the computational routine still sorts the critical points and locates points of intersection of the curves in the image. Due to the difficulties mentioned above regarding the application of the technique to solve real engineering problems, some

adaptations were made to the original method, so that it could be simplified without affecting its main attributes.

Initially, the problem domain is fully mapped. An equally spaced rectangular mesh is constructed in the domain of the problem and the value of the determinant of the Jacobian matrix at each point is calculated. Since the critical points are those in which the determinant of the Jacobian is null, the mesh is traversed, and each time changes in the signal of the determinant are identified, an arbitrary point of the segment between the two points of the mesh with distinct signals is taken as initial guess of the root calculation. Therefore, a Newton-type routine is executed until the critical point within the segment of the mesh is obtained.

The previous procedure is executed until all the mesh is traversed, that is, until all the critical points of the domain are obtained, forming the critical set. The mesh must be sufficiently refined so that the whole set of critical curves can be obtained, with the desired accuracy. After obtaining the set  $\mathcal{C}$  of critical curves, the set of critical images  $F(\mathcal{C})$  follows by calculating the value of the function of each of the critical points contained in  $\mathcal{C}$ .

### **Creation of the bank of solved points**

The bank of solved points is a set of points in the image where all their respective pre-images in the domain are known since they have been carefully computed. These points are then used as initial guesses for the process of inversion of an arbitrary point in the image of the function. The bank of solved points can be as extensive as desired and obtaining the pre-images of each of the points can be performed by the continuation method (when at least one pre-image is known) or by using a numerical method capable of getting the whole set  $p_a$  when  $F(p_a) = q_a$ . Since the inversion method can fail if it approaches sufficiently close to the critical set, it is instrumental the creation of a bank of solved points, to effectively be able to solve the system of equations in general. It is a set of points in the image where all their respective pre-images in the domain are known.

Once the bank of solved points has been built, it is needed to adopt an appropriate criteria in choosing the point that is used as the beginning point in the path created by the continuation method. Originally, the technique adopts different criteria based on the following properties: the calculated segments in the inversion process should stay away from critical points, especially from the cusp type, which are difficult to obtain pre-images. In addition, the segments should have few intersections with  $F(\mathcal{C})$ , due to the possible degeneration of solutions. Also, segments should be as short as possible. However, due to difficulties the criterion assumed for the choice of the bank point that will be taken as the initial guess of the continuation process in the inversion step is the calculation of the shortest path, since the critical points are not classified in the step of obtaining the critical curves and it is intended to avoid that the segment crosses the critical curve. In this way, the point  $q_0$  of the bank with the least Euclidean distance in relation to  $q$  — the point to be inverted — is chosen.

Choosing the point that will generate the shortest path does not guarantee that the segment will not cross some critical curve. If  $q_0$  is located on a different tile than  $q$ , the inversion process may have problems, since the segment will necessarily cross some image of a critical or boundary curve before  $q$  is reached. Therefore, it is convenient that the bank of solved points be formed by points contained in different tiles, according to the problem solving requirements.

From the point of view of user interference in relation to each of the steps of the method, the creation of the bank of solved points is the most costly stage, especially when they are very extensive and there are several pre-images, according to each specific problem. However, the homotopy-continuation technique used in the inversion step (see more in Allgower and Georg<sup>12</sup>) allows the use of a single bank in solving different problems of the same genre, that is, with variation of parameters, as shown in Guedes et al.<sup>9</sup>, which solved the double azeotropy problem of the system composed of benzene + hexafluorobenzene at different values of the system pressure, with the same bank of solved points generated at  $P = 20 \text{ kPa}$ .

## Inversion of an arbitrary point

The calculation of the pre-images is accomplished through the creation of L-shaped paths using the Euler-Newton continuation method. Initially, the element  $q_0$  of the bank of solved points in the image that is closest to the point to be inverted  $q$  is selected. Then, the points are connected to each other through two perpendicular segments, joined by their ends, going from  $q_0$  to  $q$ , which produces an intermediate point, called  $\tilde{q}$ . The respective path in the domain will be traversed through the continuation method, starting from  $p_0$ , that is, the point of the bank of solved points in the domain referring to  $q_0$ . Since each point of the image stored in the bank must have all of its respective pre-images also kept in the bank, the inversion step must be executed as many times as there are entries stored in the bank of solved points in the domain relative to  $q$ , in order that all the solutions of the system are found, producing different L-shaped paths, which start from the same initial guess.

The predictor-corrector method used to trace the L-shaped path is based on homotopy techniques. In a rudimentary way, take  $F : \mathbb{R}^n \rightarrow \mathbb{R}^n$  a smooth map. In an attempt to find the values of  $p$  that determine the solutions of  $F(p) - q = 0$ , numerical methods may fail when no prior knowledge of  $F$  is known and the initial guesses taken may not be good enough to solve the problem. One way to avoid this kind of problem is to deform the original function through a homotopy technique and try to trace an implicitly defined curve in order to reach the solution of the system through a starting point.

The scheme used in the continuation method employs the Euler's method in the predictor step and, in turn, the Newton's method is responsible for the refinement of the predicted solution in the corrector step. After calculating a point that approximates the curve of interest in each of the iterations of the predictor-corrector method, a stepsize adaptation strategy is adopted for the next iteration. It is convenient to adopt strategies of this type to avoid regions that contain singularities or to prevent the numerical method from making big jumps during the calculation of the curve. Using this artifice, it is also possible to perform a complementary evaluation of the convergence of the method. Details about method

implementation will not be described here. All information about the computational routines used in the inversion step can be found in Allgower and Georg<sup>12</sup>.

## Numerical Results

The methodology of numerical inversion of two-variable functions, adapted from Malta et al.<sup>8</sup> which considered the special case of functions from the plane to the plane, is employed in this phase equilibrium calculation. Some details regarding the construction of the bank of solved points and the numerical steps of the inversion process are given by Libotte et al.<sup>10</sup>. We present an in-depth analysis of the quantity of pre-images in limit-situations (for instance, when the critical image is approached). Furthermore, we present the thermodynamic calculation of the critical points for the binary mixture ethane + limonene for the entire range of compositions. It will also be discussed the relation of the system temperature variation with the mathematical critical curves and the possibility of using a single bank of solved points for the resolution of several different systems.

As already mentioned, the results that will be presented here were obtained essentially from systems (as described in Equation 2) with three different configurations. In the first case, when the temperature of the system is  $T = 307.4$  K and the molar fraction in the vapor phase of the ethane is set at  $y_1 = 0.998966$ , the limit situation of inversion of a point arbitrarily close to the critical image will be evaluated and the degeneracy condition solutions will be analyzed. Under these conditions, some peculiar aspects about critical curves will also be shown. Furthermore, the degeneracy of solutions will also be examined from the point of view of the simultaneously resolution of two systems with different temperatures, in order to explain the disappearance of solutions under critical conditions. For this analysis, the system temperatures  $T = 304.5$  K and  $T = 280$  K will be taken, so that the molar fraction of ethane in the vapor phase is the same in both systems.

Table 1 presents the compositions and pressures for the dew point calculation in the

system ethane + limonene at  $T = 307.4$  K and  $y_1 = 0.998966$ , where the “double-dome” structure appears, with four dew point pressures (and compositions of the liquid phase), as shown in Figure 1. The table also lists the results obtained by the method of inversion of functions from the plane to the plane for the phase equilibrium calculation problem when  $T = 304.5$  K and  $T = 280$  K, both fixed  $y_1 = 0.99945$ , where a “S” shape dew curve appears, with three and one physical roots, respectively.

Table 1: Dew point compositions and pressures for all cases studied.

Roots	$T = 307.4$ K		$T = 304.5$ K		$T = 280$ K	
	$y_1 = 0.998966$		$y_1 = 0.99945$			
	$x_1$ (mol/mol)	$P$ (kPa)	$x_1$ (mol/mol)	$P$ (kPa)	$x_1$ (mol/mol)	$P$ (kPa)
1	0.1567	619.3	0.3064	1209.4	0.0736	175.4
2	0.9829	4859.5	0.8442	3900.9	—	—
3	0.9918	4931.2	0.9917	4671.6	—	—
4	0.9979	5007.3	—	—	—	—

One can note that considering the data of the first case presented in Table 1, that one solution corresponds to a low pressure root (root 1) and the others are high pressure roots (which are close to each other). From the point of view of the calculation techniques — using classical numerical methods, such as Newton-Raphson methods — we are interested in robust methodologies capable not only to find all roots, but also to find the high pressure roots in a robust way. In order to better understand the geometry of the non-algebraic system of equilibrium, we consider some modified problems (perturbed versions of the original one) — which bear no immediate physical meaning — and use the same numbering of the roots (1 to 4).

## Thermodynamic critical point calculations

Here we present the critical curve for the mixture ethane + limonene for the entire range of compositions. As reported previously, the term “critical curve” can exhibit two different

meanings: the mathematical and the thermodynamic. Here we deal with thermodynamic critical points, and we use the approach of Heidemann and Khalil<sup>13</sup>, with a double-loop structure in temperature-molar volume, for the critical point calculation.

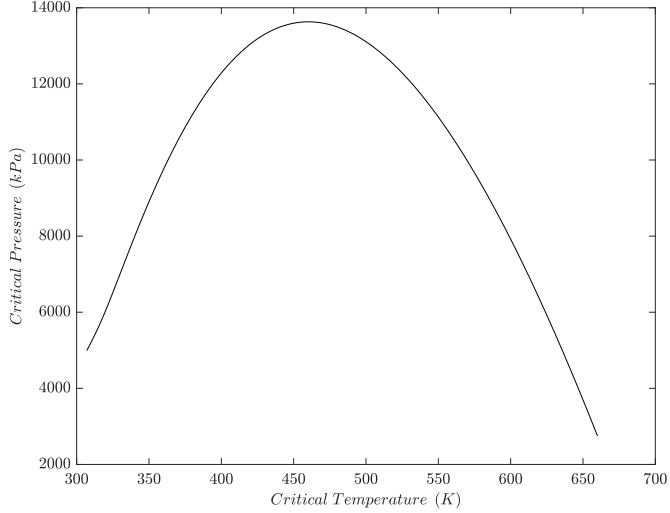


Figure 2: The thermodynamic critical curve in the system ethane + limonene.

Figure 2 illustrates the critical curve, in the temperature-pressure plane, for the mixture at hand. We observe a continuous and unique curve connecting the two pure components. Thus, this system can be classified as Type I, accordingly to the classification of binary mixtures of Van Konynenburg and Scott.<sup>14</sup> Thus, it is clear that there is no obvious relationship between the thermodynamic critical curve and the loci of singularities of the Jacobian matrix.

## Results at $T = 307.4$ K and $y_1 = 0.998966$

### An in-depth examination of the critical curves

Here, we present a deeper analysis of the mathematical critical curves in this system. Clearly, we note that — in the highlighted region — the critical curves exhibit one self-intersection, as shown in Figure 3. Furthermore, the two critical curves show a “quasi-tangent” point (or a meeting point).

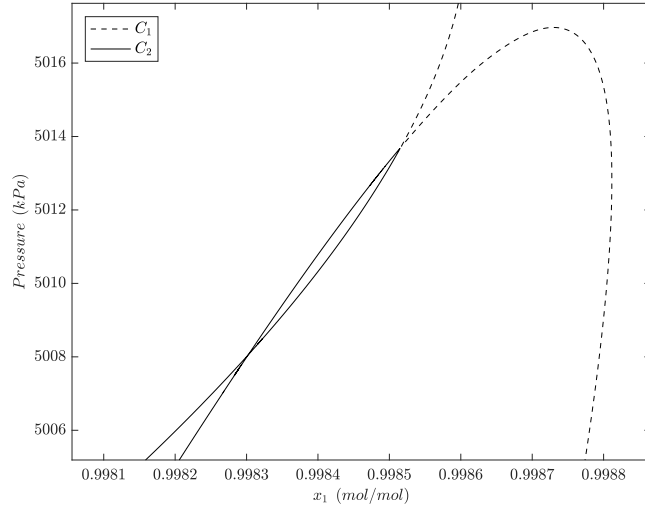


Figure 3: A detailed view of the critical curves.

An amplification of the region in the neighborhood of the “quasi-tangent” point, using a color pattern (in order to clarify the relationship between domain and image) is presented in Figure 4.

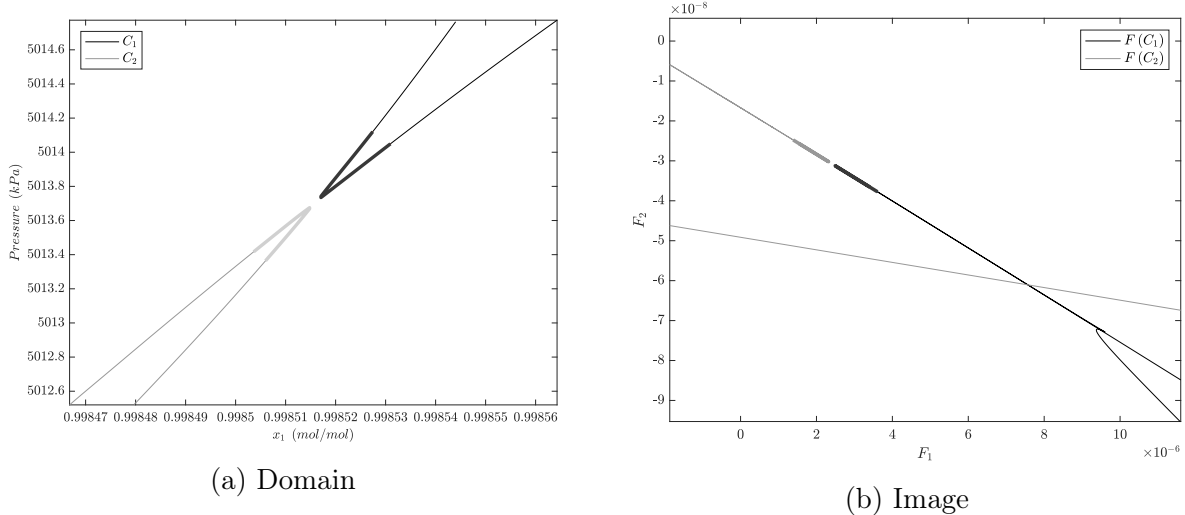


Figure 4: Amplification of the interest region of the critical curve and the critical image.

Critical images can intercept each other, although the critical curves in the domain are disjointed, such as the hypothesis suggested by Malta et al.<sup>8</sup>. In the same work, the authors also carried out an analysis of the change in the number of solutions of  $2 \times 2$  systems of nonlinear equations (the degeneration of solutions) in the vicinity of points that are folds,

cusps and those that present intersection in the image.

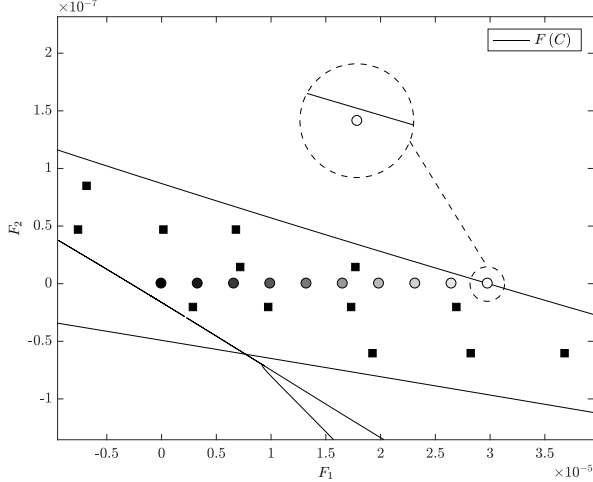
### Inversion process — approaching to the critical image

Since the mathematical critical curves represent the set of points at which the value of the determinant of the Jacobian matrix is equal to zero, it is expected that the numerical method may have problems approaching these curves continuously until the degeneracy condition occurs, that is, a change in the quantity of their pre-images — and therefore the solutions of the problem — because of the collapse of solutions at a certain point in the critical curve. This occurrence helps to explain some cases of divergence of numerical methods based on derivatives.

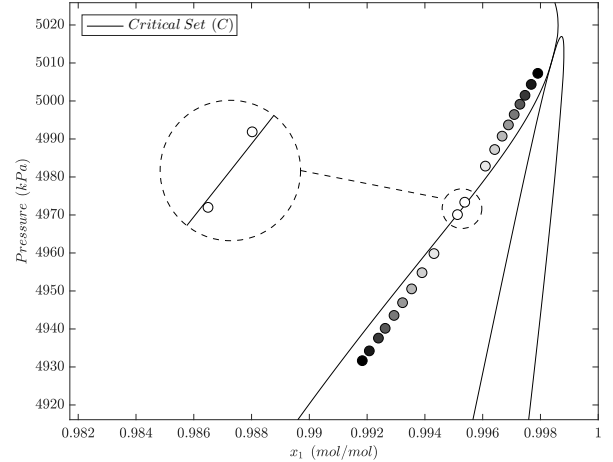
Due to the nonlinearity of the problem, all the pre-images of a set of points in the image were obtained through the method of inversion of functions from the plane to the plane. The set of points in the image were arranged from  $q = (0, 0)$  to a point sufficiently close to the critical image, equally spaced from each other and displaced only in the horizontal direction. In addition, each of the points in the image was identified by one color (in grayscale) and their respective pre-images received the same color for all four sets of solutions mentioned above. Through this scheme, it was possible to analyze the behavior of the solutions in the domain and to estimate how close a pre-image of a given point  $q$  in the image approaches a critical curve, as  $q$  approaches the critical image.

Figure 5a presents the sequence of points inverted in the image. The squares in the figure are the bank of solved points. In this situation, four pre-images are observed (in accordance with the number of solutions of the original nonlinear problem). Obviously, these solutions are not roots of the original problem, since we have  $q = (0, 0)$  for the physical nonlinear problem. On the other hand, as pointed previously, we maintain the same numbering of the roots (1 to 4).

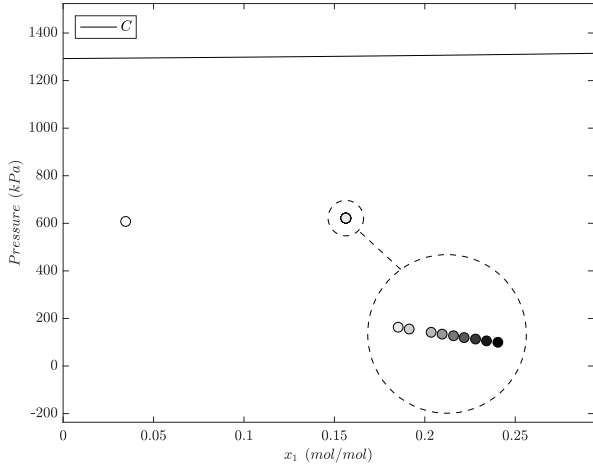
The sequences of inverted points — in the domain — for roots 3 and 4 (high pressure roots) are represented by Figure 5b. The end point of each of the sequences, that is, the one



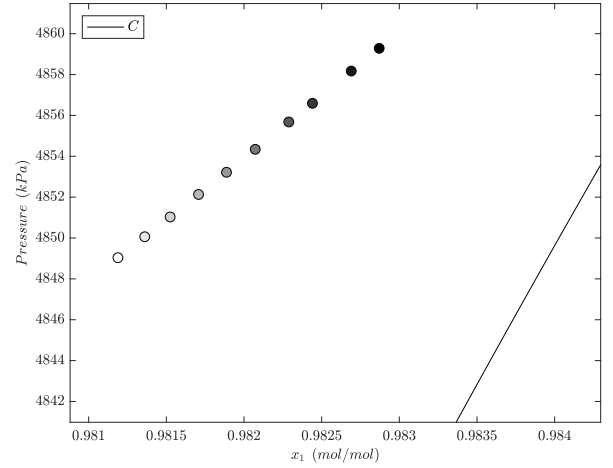
(a) Sequence of inverted points in the image.



(b) Sequences of inverted points in the domain for roots 3 and 4.



(c) Sequence of inverted points in the domain for root 1.



(d) Sequence of inverted points in the domain for root 2.

Figure 5: Sequence of points that have been inverted and their respective pre-images, identified by similar colors.

in which the pre-image moves closer to the critical curve (represented by the white color), is being shown in detail by zooming. We can clearly observe the occurrence of a degeneration scenario: two solutions collapsing simultaneously to the same point of the critical curve. It should be noted that the points can be as close as desired to the critical set, which depends on the level of approximation that has been used, since the continuation method does not cross the critical curve during the inversion process. However, it is possible to estimate the point of the critical curve in the domain in which the points of each of the sequences will

degenerate. Just draw a straight line which connects to each other, and check what is the intersection point between this line and the critical curve. On the other hand, Figures 5c and 5d contain the sequence of inverted points regarding roots 1 and 2, respectively. In these cases, the inverted points are not close to the critical curves.

Another very important factor to be considered is the positioning of the elements of each of the calculated pre-image sequences. In order for solution degeneration to occur, the degenerated points must be located on different tiles. As one point in the image approaches a critical image, two of its respective pre-images may approach a critical curve. According to Malta et al.<sup>8</sup>, the scenario that characterizes the degeneracy of solutions in pairs, as is the case of the problem studied, is that the solutions are approaching the vicinity of a critical point of the fold type. The creation of a robust bank of solved points is also essential in this analysis, since it would not be possible to calculate the correct pre-images if the inversion method took as an initial guess a point in the bank of solved points in the domain that was located on a different tile than the one in which the desired solution is.

Hereafter, we detail the inversion process for the point close to the critical image. Figure 6a indicates the L-shaped path in the image. Again, the square represents a point in the bank of solved points and the desired point, namely, the point to be inverted, is represented by a circle with the corresponding color. In turn, the paths in the domain are detached in Figure 6b. One can note that the L-shaped paths were deformed and are virtually straight lines. This is due to the critical image of the system limiting the tile where the point to be inverted is located in a very restricted area. With this, the bank of solved points must be relatively close to the point to be inverted (besides the fact of taking the point contained in the bank that is closest to the point to be inverted as initial guess) and the method of continuation reaches the pre-image through an almost straight path. Once again, the degeneration process is clearly indicated and the critical curve has a fold at this point.

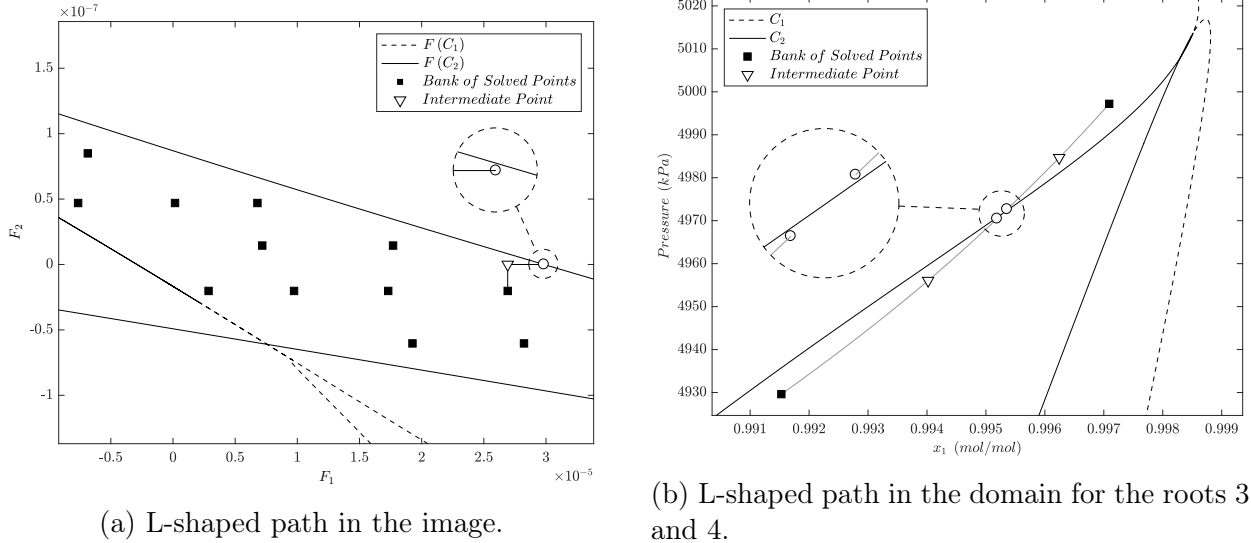


Figure 6

## Results at $T = 304.5$ K and $T = 280$ K, with $y_1 = 0.99945$

In the case analyzed previously, the degeneracy of two of the system solutions around a fold was clear when the point to be inverted was sufficiently close to the critical image. Now, two cases will be analyzed simultaneously, such as each of the systems, through only the variation of their temperature, presents different quantities of solutions. The objective is to show the exact moment in which the degeneration of two solutions of the problem occurs, but due to the proximity of the solutions to the critical set. Here, the same strategy of the previous case will be used to obtain the results: a sequence of points in the image will be inverted, from a known point (for instance,  $q = (0, 0)$ ) to a point sufficiently close to the critical image, without being crossed. Thus it is possible to observe the behavior of the solutions in the domain of the problem.

At  $T = 304.5$  K and  $y_1 = 0.99945$ , the dew point curve still exhibits a double retrograde behavior, but now the curve has a sigmoidal shape (instead of a double dome). In this situation, we observe three dew point pressures (and liquid compositions) for a narrow range of molar fractions. This time, the system has two solutions at high pressures and one under reduced pressure. In addition, the distance between the solutions, in terms of pressure, is

relatively higher than in the previous case.

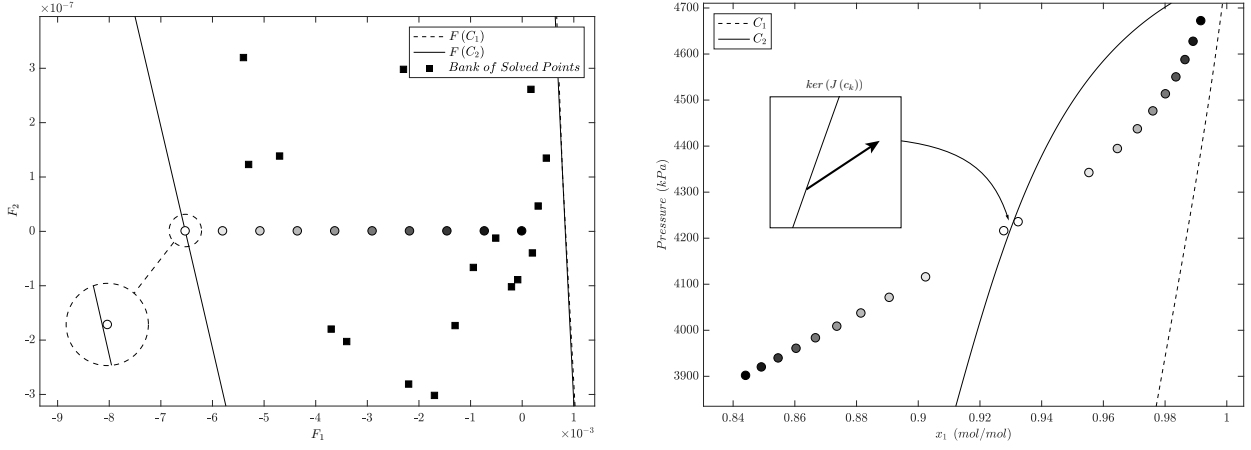
### Inversion process — approaching the critical image

Figure 7a shows the sequence of points in the image to be inverted, from  $q = (0, 0)$  to a point sufficiently close to the critical image. Following the same trend, the points in the image were identified by distinct colors, and their pre-images respected the established organization. The bank of solved points was randomly arranged in the image and each of its pre-images was obtained. In relation to the previous problem, it is not possible to use the same bank of solved points, since two parameters were varied, temperature and pressure, what makes the system have absolutely different thermodynamic characteristics. The zoom in Figure 7a shows that the white point does not intersect or even cross the critical image.

Figure 7b shows the behavior of each of the pre-images, for the two solutions at high pressures (roots 2 and 3), obtained through the method of inversion of functions from the plane to the plane. As expected, the behavior of the sequence of pre-images of the two solutions in question suggests that as we approach the critical image two solutions approach the critical curve until both collapse in a given point of the critical curve. This behavior characterizes the degeneracy of solutions.

It is known that, according to the definition, one of the conditions for characterizing a critical points of the fold type is that the kernel of the Jacobian matrix at the critical point does not coincide with the vector tangent to  $\mathcal{C}$  at the same point. In Figure 7b, the critical point at which degeneration occurs is estimated and denoted by  $c_k$ . The approximation was performed by interpolating between the sequence of pre-images and  $c_k$  is a point of the critical curve that was crossed by the interpolated curve. The accuracy of the  $c_k$  approximation is not significant, since it is conjectured that there are only folds in the vicinity of  $c_k$ . Therefore, the kernel of the Jacobian matrix in  $c_k$  was obtained and, through the analysis of Figure 7b, it is clear that this vector does not coincide with the vector tangent to  $\mathcal{C}$  in  $c_k$ .

In turn, Figure 8 illustrates the L-shaped path of the inversion process in the domain to



(a) Sequence of inverted points (image) for  $T = 304.5$  K and  $y_1 = 0.99945$ .

(b) Sequence of inverted points (domain) for  $T = 304.5$  K and  $y_1 = 0.99945$  (Roots 2 and 3).

Figure 7

the last point of the sequence in the image (the one closest to the critical image, marked in white in Figure 7a). Again, we observed that the two pre-images, corresponding to roots 2 and 3, tend to degenerate into a single pre-image. In addition, one can note the importance of knowing the critical set of the problem and, consequently, the tiles that form the domain of the system. They define the points of singularities that may cause problems to the continuation method in the process of creating the L-shaped path of the inversion step and consequently provide the analysis of the degeneracy of solutions.

The use of the bank of solved points of the previous problem would not be possible in this problem because, in addition to the number of distinct pre-images in each of the problems, possibly the points of the bank of solved points in the domain could be located in tiles different from the desired pre-images. Since the points contained in the bank act as the initial guess for the method of continuation in the inversion step, the L-shaped path would necessarily cross the critical curve of the problem, which could cause an error in the computational routine.

Finally, Figure 9 shows the L-shaped path of the problem at  $T = 280$  K and  $y_1 = 0.99945$ . Under such conditions, the problem has only one solution, despite the sigmoid behavior, as can be seen in Figure 1.

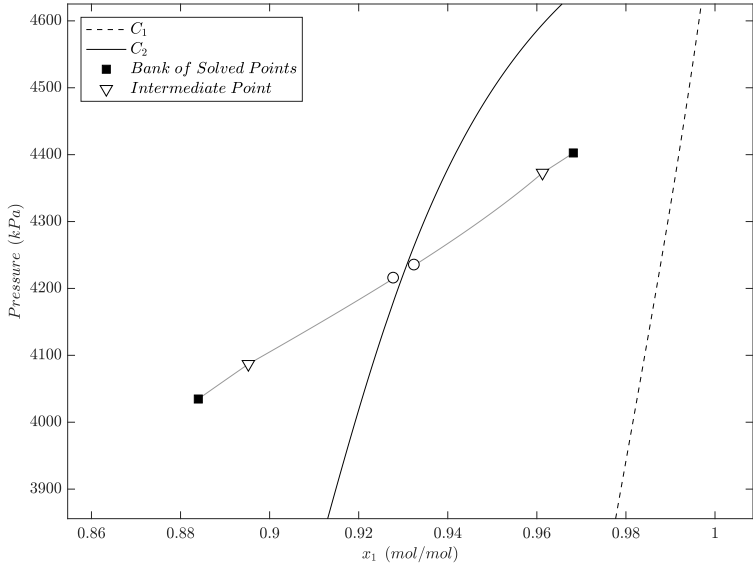


Figure 8: The L-shaped path in the domain, Roots 2 and 3, for  $T = 304.5$  K and  $y_1 = 0.99945$ .

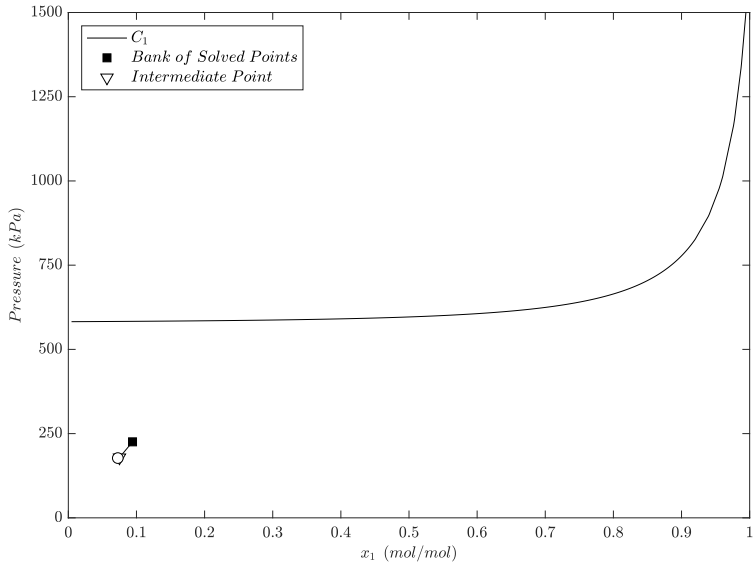


Figure 9: The L-shaped path in the domain, Root 1, for  $T = 280.0$  K and  $y_1 = 0.99945$ .

## The influence of temperature on the critical curve

The last resource to be investigated in this work corresponds to the influence of the system temperature (specified) on the critical curve. Obviously, the phenomenon of double retrograde vaporization is a function dependent on the temperature of the system. Since the

critical curves have a direct influence on the process of obtaining pre-images — the system solutions — the analysis of the variation of the temperature of the system is essential in the resolution of systems of this type. The behavior of the critical curves under different values of the system parameters (in this case, the temperature) can clarify the occurrence of numerical errors in nonlinear system resolution techniques.

To perform the tests, the critical sets of the systems were obtained by fixing the molar fraction of the ethane vapor phase at  $y_1 = 0.99966$  and varying the system temperature from  $T = 299$  K to  $T = 300$  K, as can be seen in the dew point curves shown in Figure 10b. In this way, it was possible to evaluate the behavior of the critical images of the system, varying only one of the parameters of the model, so that all systems analyzed had the same number of pre-images when  $q = (0, 0)$ .

In Figure 10a, it is possible to observe the influence of the system temperature variation on the behavior of the critical images (and therefore the variation of the critical curves in the sense of the solutions degeneration) in the vicinities of  $q = (0, 0)$ . As the temperature of the system decreases, its critical image is ever closer to  $q = (0, 0)$ . The closer the critical image is to the point to be inverted, the more limited will be the performance of the numerical method used to obtain the results, since it increases the chances of crossing the critical curve.

When the molar fraction of the vapor phase of ethane is fixed, the system obviously no longer has three distinct solutions, in the case studied, when defining a temperature that carries a behavior like that shown by the dew point curve calculated at  $T = 298$  K in Figure 10b. However, the case treated here predicts that, for a given system temperature, a certain segment of the critical image may be so close to  $q = (0, 0)$  that it would be very difficult to obtain the pre-images of the system if the derivatives were evaluated sufficiently close to the point where the pre-images are desired.

Still considering the context of the system temperature variation, fixing the molar fraction of the vapor phase of the solvent, it will be presented the numerical results on the resolution capacity of different systems using a single bank of solved points. As already mentioned, the

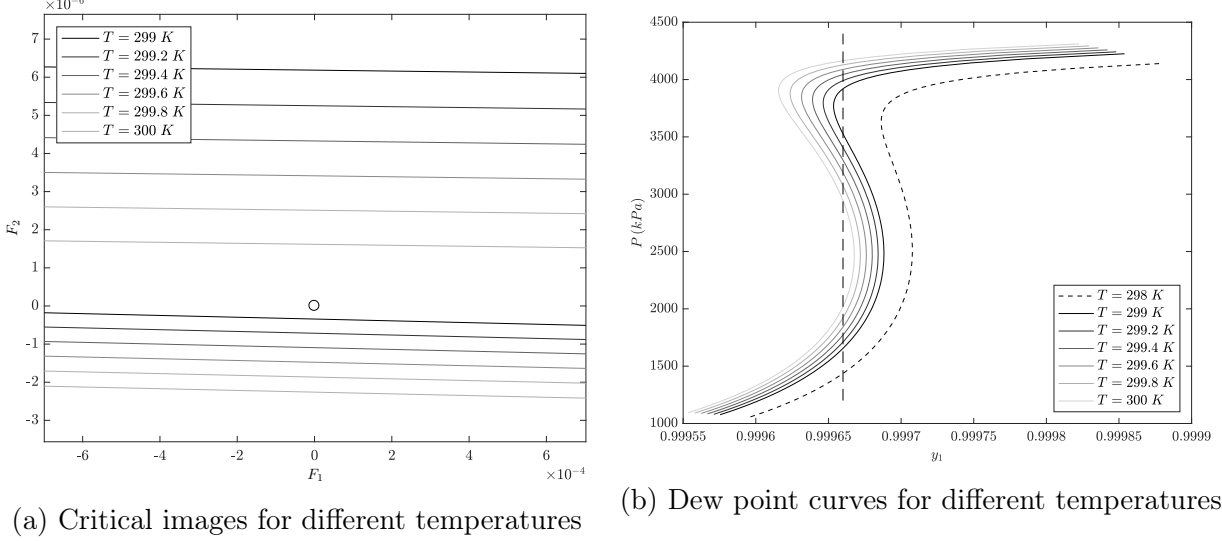


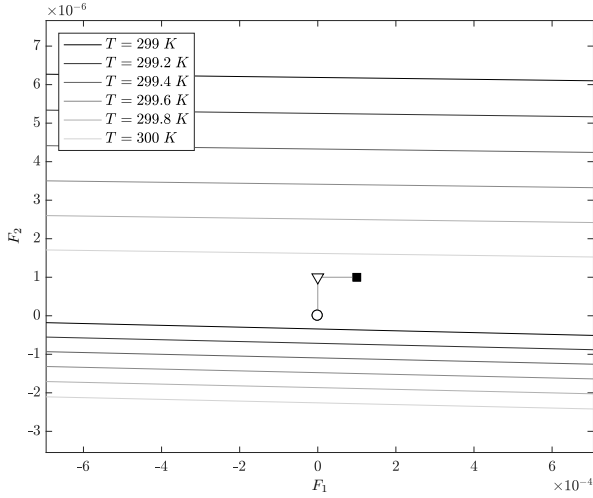
Figure 10: Influence of system temperature variation on the critical images of the problem. The molar fraction of the vapor phase of ethane is set at  $y_1 = 0.99966$  for all cases, as shown in the dashed line.

creation of the bank of solved points is the most costly step from the point of view of user interference in a step of the numerical method. Therefore, one must consider the possibility of creating a robust bank of solved points in order to minimize the effort required in this step.

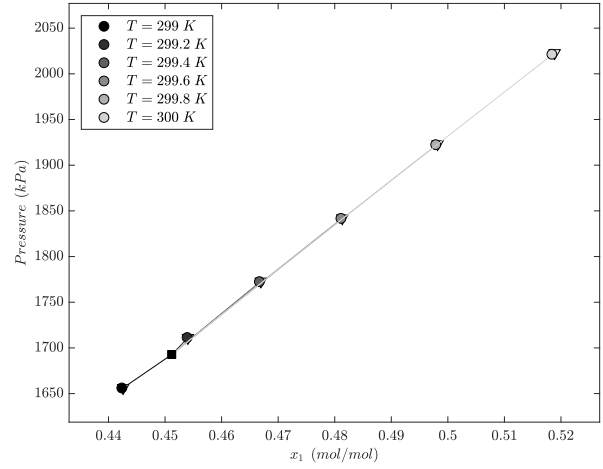
Of course, the robustness of the bank of solved points does not mean strictly that the larger the amount of pre-images stored, the better the quality of the bank of solved points. One should consider the fact that the inversion step evaluates the distance between each point stored in the bank of solved points in the image and the point to be inverted. Thus, high amounts of stored points can cause slowness in the process. On the other hand, bank of solved points containing many elements can mean that they are located on different tiles, which increases the chances of success in performing the inversion step. In general, to use a single bank of solved points to obtain the pre-images of a number of distinct problems (under the circumstances already specified), the condition of using a point as the initial guess that is on the same tile in all problems must be satisfied.

Figure 11a shows the L-shaped path in the image of the inversion process of the point

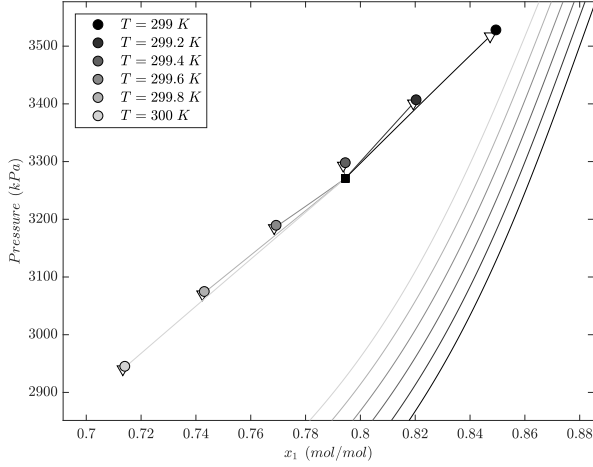
$q = (0, 0)$  for all the problems analyzed. The point of the bank of solved points (represented by the black square), was obtained using the system at  $T = 299$  K, and used in the inversion process of all systems. Note that the tile on which the point of the bank of solved points in the image and the point  $q$  are located is the same, in all cases. In turn, Figures 11b – 11d show the L-shaped paths in the domain, referring to each root of the problems, with the system temperature specified. The similarity of colors identifies the respective points in the



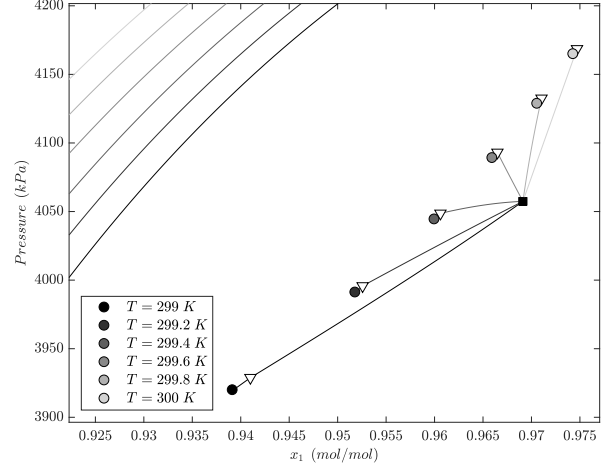
(a) L-shaped path in the image for the inversion of all points using the same bank of solved points.



(b) L-shaped paths in the domain referring to root 1 of each of the systems.



(c) L-shaped paths in the domain referring to root 2 of each of the systems.



(d) L-shaped paths in the domain referring to root 3 of each of the systems.

Figure 11: All solutions of the systems varying from  $T = 299$  K to  $T = 300$  K, with  $y_1 = 0.99966$ , using the same bank of solved points, obtained for the system at  $T = 299$  K.

domain and image. Note that the inversion process — the creation of the L-shaped path — always starts from the same point of the bank of points solved, created with  $T = 299$  K. In the results shown in Figure 11, only the point closest point contained in the bank of solved points in relation to  $q$  is shown. The other points were omitted.

In all the results obtained, the use of a single bank of solved points had no adverse effect in obtaining results with the accuracy defined in the continuation predictor-corrector method. The roots were obtained with satisfactory accuracy, similarly to the case when the inversion process is performed with the bank of solved points created using the same temperature of the system in which it is desired to obtain the pre-images. However, the observed difference is that, in general, the method trace a longer path until solutions are obtained. However, there are cases in which the point bank of solved points in the domain may be located closer to the desired root, due to the non-linearity of the system. Therefore, this approach can be understood as the use of a “non-ideal” initial guess in the numerical inversion process.

## Conclusions

In this work we investigated some numerical details of the mathematical structure of the calculation of dew points in a thermodynamic system with double retrograde phenomenon (4 or 3 dew points in a narrow range of compositions), using a robust numerical strategy — the numerical inversion of functions. Despite the apparent ease of solving a nonlinear system of algebraic equations with two equations and two unknowns, the occurrence of the double retrograde vaporization phenomenon in the phase equilibrium problem inserts a considerable degree of complexity into the system, motivating the need for a more in-depth analysis of the problem studied and the use of consistent numerical methods for the analysis of singular situations. Despite the difficulty of applying the complex theorems that support the inversion method in engineering problems and, specifically, in the problem studied here, the technique is very efficient, since satisfactory results have been obtained, even with the

needs of adaptation of specific steps in the technique.

By analyzing the behavior of the critical set, mainly with the temperature variation of the system, it was possible to identify regions where the solution no longer exists, when the point to be inverted in the image is sufficiently close to the critical set. Consequently, it is possible to predict the regions where, possibly, numerical methods based on derivatives may have problems of convergence. Besides that, the study of solution degeneration provides a comprehensive amount of information about the system and its behavior about complex regions.

It was observed that, at least in the cases studied, degenerate solutions were always those with the highest pressure value. This tendency occurs because, in general, the higher pressure solutions are more unstable (from a mathematical point of view). Particularly during the occurrence of the double-dome phenomenon of double retrograde vaporization, the upper dome occurs under a very narrow range of molar fraction and pressure in the vicinity of high pressure solutions. Under small variations of the system temperature, the double dome ceases to exist and the dew point curve takes the sigmoidal form. This fact explains the occurrence of degeneration of solutions that are usually at high pressures.

## Acknowledgement

The authors thank to the Brazilian agencies Coordination for the Improvement of Higher Education Personnel (CAPES) and the Carlos Chagas Filho Foundation for Research Support in the State of Rio de Janeiro (FAPERJ) for providing partial financial support to conduct this research.

## References

- (1) Chen, R. J. J.; Chapplear, P. S.; Kobayashi, R. Dew point loci for methane-n-butane binary system. *J. Chem. Eng. Data* **1974**, *19*, 53.

- (2) Chen, R. J. J.; Chapplear, P. S.; Kobayashi, R. Dew point loci for methane-n-pentane binary system. *J. Chem. Eng. Data* **1974**, *19*, 59.
- (3) Raeissi, S.; Peters, C. J. On the phenomena of double retrograde vaporization: multi dew point behavior in the binary system ethane + limonene. *Fluid Phase Equilib.* **2001**, *191*, 33.
- (4) Raeissi, S.; Peters, C. J. Simulation of double retrograde vaporization using the Peng-Robinson equation of state. *J. Chem. Thermodyn.* **2003**, *35*, 573.
- (5) Peng, D.; Robinson, D. A new two-constant equation of state. *Ind. Eng. Chem. Res.* **1976**, *15*, 59.
- (6) Raeissi, S.; Peters, C. J. Thermodynamic analysis of the phenomenon of double retrograde vaporization. *J. Phys. Chem. B* **2004**, *108*, 13771.
- (7) Platt, G. M.; Bastos, I. N.; Domingos, R. P. Calculation of double retrograde vaporization: Newton's methods and Hyperheuristic approach. *J. Nonlin. Sys. Appl.* **2012**, *3*, 107.
- (8) Malta, I.; Saldanha, N. C.; Tomei, C. The Numerical Inversion of Functions from the Plane to the Plane. *Math. Comput.* **1996**, *65*, 1531.
- (9) Guedes, A. L.; Moura Neto, F. D.; Platt, G. M. Prediction of Azeotropic Behaviour by the Inversion of Functions from the Plane to the Plane. *Can. J. Chem. Eng.* **2015**, *93*, 914.
- (10) Libotte, G. B.; Neto, F. D. M.; Guedes, A. L.; Platt, G. M. Robust Prediction of Double Retrograde Vaporization by Numerical Inversion of Functions. *Int. Rev. Mech. Eng.* **2016**, *10*, 452.
- (11) Malta, I. P.; Saldanha, N. C.; Tomei, C. *Geometry and Numerical Analysis of functions*

*from the plane to the plane* (in Portuguese); Instituto de Matemática Pura e Aplicada, 1993.

- (12) Allgower, E. L.; Georg, K. *Numerical Continuation Methods: An Introduction*, 1st ed.; Springer Series in Computational Mathematics 13; Springer-Verlag Berlin Heidelberg, 1990.
- (13) Heideman, R. A.; Khalil, A. M. The calculation of critical points. *AICHE J.* **1980**, *26*, 769.
- (14) Van Konynenburg, P. H.; Scott, R. L. Critical lines and phase equilibria in binary van der Waals mixtures. *Philos. Trans. R. Soc. London, Ser. A* **1980**, *298*, 495.

## Graphical TOC Entry

Some journals require a graphical entry for the Table of Contents. This should be laid out "print ready" so that the sizing of the text is correct. Inside the `tocentry` environment, the font used is Helvetica 8 pt, as required by *Journal of the American Chemical Society*. The surrounding frame is 9 cm by 3.5 cm, which is the maximum permitted for *Journal of the American Chemical Society* graphical table of content entries. The box will not resize if the content is too big: instead it will overflow the edge of the box. This box and the associated title will always be printed on a separate page at the end of the document.